Iranian Journal of Basic Medical Sciences
ijbms.mums.ac.ir

Norepinephrine promotes the proliferation, migration, and phenotypic transformation of renal artery vascular smooth muscle cells via ROCK1

Sixuan Chen [1, 2#], Lina Wang [2#], Lu Wang [2], Hui Li [2], Junyao Lu [3], Yaxin He [2], Yihong Zhang [4], Yuanyuan Guo [1, 2, 3*], Mingyu Liu [1, 3*]

[1] Department of Cardiology,The First Affiliated Hospital, Harbin Medical University, Harbin 150088, China
[2] Department of Geriatrics,The First Affiliated Hospital, Harbin Medical University, Harbin 150088, China
[3] The Key Laboratory of Cardiovascular Disease Acousto-Optic Electromagnetic Diagnosis and Treatment in Heilongjiang Province, The First Affiliated Hospital, Harbin Medical University, Harbin 150088, China
[4] Department of endocrinology, Heilongjiang Province Hospital, Harbin 150088, China

ARTICLE INFO

Article type:
Original

Article history:
Received: Aug 20, 2025
Accepted: Oct 27, 2025

Keywords:
Hypertensive nephropathy
Mitochondrial fission
Norepinephrine
Rho-associated kinase
Vascular smooth muscle-cells

ABSTRACT

Objective(s): This study investigated the role of norepinephrine (NE) and ROCK1 in regulating renal artery vascular smooth muscle cells (rVSMCs).

Materials and Methods: rVSMCs were treated with NE, and ROCK1 expression was assessed. Cell proliferation, migration, and phenotypic switching were evaluated using EdU incorporation and wound-healing assays. ROCK1 was silenced by siRNA. Mitochondrial membrane potential and morphology were analyzed to determine NE-induced mitochondrial alterations.

Results: NE significantly up-regulated ROCK1 expression in rVSMCs. It promoted proliferation, migration, and phenotypic switching, as indicated by increased expression of proliferative and migratory markers, whereas ROCK1 silencing attenuated these effects. NE also reduced mitochondrial membrane potential and induced mitochondrial fission, suggesting an additional mechanism contributing to vascular remodeling.

Conclusion: NE promotes rVSMCs proliferation, migration, and phenotypic switching through ROCK1 activation and alters mitochondrial dynamics. These findings identify the NE–ROCK1 axis as a critical mediator of vascular remodeling in hypertensive nephropathy and suggest it may serve as a promising therapeutic target.

▶Please cite this article as:
Chen S, Wang L, Wang L, Li H, Lu J, He Y, Zhang Y, Guo Y, Liu M. Norepinephrine promotes the proliferation, migration, and phenotypic transformation of renal artery vascular smooth muscle cells via ROCK1. Iran J Basic Med Sci 2026; 29: 605-612. doi: https://dx.doi.org/10.22038/ijbms.2026.90472.19527

Introduction

Cardiovascular disease is the leading cause of mortality worldwide, with hypertension serving as a major contributing risk factor (1, 2). Long-term hypertension causes irreversible kidney damage (3), and blocking this process may effectively alleviate disease progression. In recent years, sympathetic nerve radiofrequency ablation has been proposed as a treatment for hypertensive nephropathy, as it significantly reduces norepinephrine (NE) secretion by ablating the sympathetic nerves surrounding the kidneys (4, 5).

Norepinephrine functions as a neurotransmitter in both the central and peripheral nervous systems, and also acts as a hormone in the bloodstream. In the brain, NE regulates wakefulness, memory, and addiction (6-8). When released into the vasculature, NE increases peripheral vascular resistance by constricting vascular smooth muscle—particularly arterioles and veins—thereby elevating blood pressure (9). Under chronic pathological conditions, however, this leads to vascular remodeling, which further exacerbates hypertension and cardiovascular disease (10, 11). Accumulating evidence suggests that NE contributes to hypertensive nephropathy; however, its role in renal vascular smooth muscle cells (rVSMCs) has not been thoroughly investigated.

Rho-associated coiled-coil containing protein kinase 1 (ROCK1) is a serine/threonine kinase belonging to the Rho kinase family (12). It plays a critical role in diverse cellular functions, including autophagy, cytoskeletal dynamics, apoptosis, NETosis, and extracellular matrix production (13-15). ROCK1 is particularly important in regulating vascular smooth muscle cells (VSMCs) contraction, as it enhances contractile force by promoting myosin light chain

*_Corresponding authors:_ Mingyu Liu. Department: The Key Laboratory of Cardiovascular Disease Acousto-Optic Electromagnetic Diagnosis and Treatment in Heilongjiang Province, Institute/University/Hospital: The First Affiliated Hospital, Harbin Medical University, Street Name & Number: No.23 Youzheng Street, City, State, Postal code, Country: Harbin, China. Tel/ Fax: 15114560627, Email: liumingyu0504@126.com; Yuanyuan Guo. Department: Department of Cardiology, Institute/University/Hospital: The First Affiliated Hospital, Harbin Medical University, Street Name & Number: No.23 Youzheng Street, City, State, Postal code, Country: Harbin, China. Tel/ Fax: 15204695797, Email:guoyuanyuan@hrbmu.edu.cn
# These authors contributed equally to this work

phosphorylation (16, 17).In addition, ROCK1 plays a pivotal role in renal pathophysiology. Evidence shows that ROCK1 participates in cytoskeletal remodeling, cell adhesion, and migration in glomerular and tubular cells, and promotes renal interstitial fibrosis by driving fibroblast activation and epithelial-to-mesenchymal transition (EMT)(18-20). ROCK1 activation has also been linked to proteinuria, podocyte injury, and hemodynamic abnormalities in diabetic nephropathy (21, 22). Moreover, pharmacological inhibition of ROCK signaling, for example, through the use of ROCK inhibitors, has been shown in multiple animal models to attenuate renal fibrosis, reduce proteinuria, and preserve renal function, underscoring its potential therapeutic relevance in kidney disease (23). However, the relationship between NE and ROCK1 in rVSMCs has rarely been reported.

In the present study, we demonstrated that NE promotes the proliferation, migration, and phenotypic switching of rVSMCs by activating ROCK1. Furthermore, we found that NE affects mitochondrial dynamics in rVSMCs. Together, these findings suggest that NE and ROCK1 may represent potential therapeutic targets for hypertensive nephropathy.

Materials and Methods

Cell culture

Primary rat renal artery smooth muscle cells (CM-R061) were purchased from Wuhan Pricella Biotechnology. The cells were cultured in DMEM supplemented with 10% FBS and 1% penicillin–streptomycin in a humidified incubator maintained at 37 ˚C with 5% CO_2. rVSMCs at passages 3-6 were used for all experiments. The experimental protocol was approved by the Ethics Committee of the First Affiliated Hospital of Harbin Medical University (Approval number: 2022110).

Western blot analysis

Cells were lysed in radioimmunoprecipitation assay (RIPA) buffer supplemented with protease and phosphatase inhibitors, and the lysates were centrifuged to collect the supernatant. After washing with pre-cooled PBS, proteins were separated by SDS–PAGE (sodium dodecyl sulfate–polyacrylamide gel electrophoresis), transferred onto a PVDF membrane, and blocked with 5% BSA for 90 min at room temperature. The membranes were then incubated overnight at 4 ˚C with the indicated primary antibodies (24).

The primary antibodies included ROCK1(1:1000, 21850-1-AP, Proteintech), MMP9(1:1000, ab76003, Abcam), MMP2(1:1000, ab92536, Abcam), PCNA(1:1000, ab92552, Abcam), GAPDH(1:10000, AC033, ABclonal), OPA1(1:1000, 382025, ZENBIO), MFN1(1:1000, 66776-1-Ig, proteintech), DRP1(1:1000, 340336, ZENBIO), SM-22α(1:1000, ab155272, Abcam), α-SMA(1:1000, 250104, ZENBIO), β-actin(1:10000, AC026, ABclonal),Cyclin D1(1:1000, ab134175, Abcam). Following washing, the bands were incubated with an HRP-conjugated secondary antibody at room temperature for 1 hr and analyzed using an electrochemiluminescence (ECL) system.

Reverse transcription and real-time PCR

Simply Total RNA Extraction Kit (BioFlux, BSC52M1) was used to extract total RNA from VSMCs. cDNA was synthesized from 1 μg of total RNA. The relative RNA expression levels were quantified by qRT-PCR using SYBR Green (Roche, 573113500). Primer sequences are displayed in Supplementary Table 1. The ΔΔCT method was used to calculate relative quantities normalized to β-actin (25).

Target Primers sequence:
Actb (Rat): Forward 5'-TGTCACCAACTGGGACGATA-3'
Reverse 5'-GGGGTGTTGAAGGTCTCAAA-3'
MMP9 (Rat): Forward
5'-CCTGGAACTCACACGACATCTT-3'
Reverse 5'-GAGTGGGGGATGCTGATCTT-3'
MMP2(Rat):Forward
5'-GATACCCCTTTGACGGTAAGGA-3'
Reverse 5'-CAGTGGACATAGGGCAGCAA-3'
Cyclin D1(Rat): Forward
5'-GCTGTGCATCTACACCGACA-3'
Reverse 5'-AGGTCCACTTGAGCTTGTTCAC-3'
PCNA(Rat):Forward
5'-GTTCCCTGGAGTGTTTGCCA-3'
Reverse 5'-GCGTTTGGATGACGTGTGTC-3'
SM22α(Rat):Forward
5'-CCTGGAGAAGAGGAGCCAGA-3'
Reverse 5'-AGTCCAGGAAGGTCCCAATC-3'
α-SMA(Rat):Forward
5'-GTCCCAGACATCAGGGAGTAA-3'
Reverse 5'-TCGGATACTTCAGCGTCAGGA-3'

Transfection of siRNA (6-well plate as an example)

Small interfering RNA (siRNA) transfection was carried out using Lipofectamine™ 2000 Transfection Reagent (GlpBio, GK20005) according to the manufacturer's instructions. Rat vascular smooth muscle cells (rVSMCs) were seeded in 6-well plates and cultured overnight to reach approximately 70-80% confluence. Prior to transfection, the culture medium was replaced with 2 ml of serum-free DMEM. For each well, 100 pmol of ROCK1 siRNA duplexes or scrambled negative-control siRNA was diluted in 250 μl of serum-free DMEM and gently mixed with 5 μl of Lipofectamine™ 2000 diluted in 250 μl of serum-free DMEM. After incubation for 5 min at room temperature, the siRNA-lipid complexes were combined and incubated

Table 1. Gene-specific primer sequences used in this study

Target		Primer sequence
Actb(Rat)	Forward	5'-TGTCACCAACTGGGACGATA-3'
	Reverse	5'-GGGGTGTTGAAGGTCTCAAA-3'
MMP9(Rat)	Forward	5'-CCTGGAACTCACACGACATCTT-3'
	Reverse	5'-GAGTGGGGGATGCTGATCTT-3'
MMP2(Rat)	Forward	5'-GATACCCCTTTGACGGTAAGGA-3'
	Reverse	5'-CAGTGGACATAGGGCAGCAA-3'
Cyclin D1(Rat)	Forward	5'-GCTGTGCATCTACACCGACA-3'
	Reverse	5'-AGGTCCACTTGAGCTTGTTCAC-3'
PCNA(Rat)	Forward	5'-GTTCCCTGGAGTGTTTGCCA-3'
	Reverse	5'-GCGTTTGGATGACGTGTGTC-3'
SM22α(Rat)	Forward	5'-CCTGGAGAAGAGGAGCCAGA-3'
	Reverse	5'-AGTCCAGGAAGGTCCCAATC-3'
α-SMA(Rat)	Forward	5'-GTCCCAGACATCAGGGAGTAA-3'
	Reverse	5'-TCGGATACTTCAGCGTCAGGA-3'

Actb: Actin beta; Mmp9: Matrix metallopeptidase 9; Mmp2: Matrix metallopeptidase 2; Ccnd1: Cyclin D1; Pcna: Proliferating cell nuclear antigen; Tagln: Transgelin; Acta2: Actin alpha 2

for an additional 20 min before being added dropwise to the cells. After 6 hr of incubation, the medium was replaced with complete DMEM supplemented with 10% FBS. Cells were cultured for 24 hr post-transfection, then treated with or without norepinephrine for an additional 24 h. The target sequence of ROCK1 siRNA was 5′-GCUAUCAAGUUCUCGAUUAUU-3′(26).

Wound-induced migration assay

Cell migration was assessed using a wound-healing assay. rVSMCs (4×10^5) subjected to different treatments were seeded into 6-well plates and cultured in DMEM containing 10% FBS. When the cells reached 90-100% confluence, a scratch was made using a 200 µl pipette tip, and detached cells were removed by rinsing with PBS. The cells were then maintained in serum-free DMEM, and wound closure was monitored at 0 and 24 h. The wound-healing rate was calculated using the following formula:

Wound-healing rate (%)=[(wound area at 0h−wound area at 24 h) / wound area at 0h]×100% (27).

EdU assay

Cell proliferation was evaluated using an EdU incorporation assay (Beyotime, C0071s). rVSMCs (1.5×10^4 cells/well) were seeded into 6-well plates, subjected to the indicated treatments, and incubated with EdU reagent (1:1000 dilution) for 3 hr the following day. After fixation with 4% paraformaldehyde, the cells were stained with Hoechst and a fluorescent dye according to the manufacturer's protocol. EdU-positive cells were quantified using Photoshop software (28).

Immunofluorescence

Cells were fixed with 4% paraformaldehyde for 20 min at room temperature and washed three times with PBS. Permeabilization was performed using 0.25% Triton X-100 in PBS for 10 min, followed by blocking with 1% BSA. The cells were then incubated with the primary antibody (1:200 dilution in PBS) overnight at 4 ˚C. After three washes with PBS, the secondary antibody was applied for 1 hr in the dark. Nuclei were counterstained with 0.1% DAPI for 5 min at room temperature. Images were captured using a fluorescence microscope (29).

Measurement of intracellular calcium in rVSMCs

Intracellular calcium levels were measured using the fluorescent probe Fluo-4 AM (Invitrogen, Carlsbad, CA, USA). rVSMCs were adjusted to a density of 2×10^5 cells/ml and seeded in laser confocal dishes. After treatment under the indicated experimental conditions, Fluo-4 AM was added at a final concentration of 10 µmol/L according to the manufacturer's instructions, and cells were incubated in the dark for 30 min. The cells were then washed repeatedly with calcium-free PBS, centrifuged twice, and immediately imaged using a laser confocal microscope (30).

Electron microscopy

Electron microscopy was used to examine mitochondrial shape and localization. In short, cells were stabilized by incubation in 0.2 ml of 2× fixative (containing 3% paraformaldehyde and 2.5% glutaraldehyde in 0.1 M cacodylate buffer) for 1 hr at room temperature. After centrifugation at 3000 RPM for 10 min at 30 ˚C, the cells were rinsed with 0.1 M cacodylate buffer and then stained for 20 min with Evans Blue solution. The cell suspension was centrifuged again for 10 min at 3000 RPM with the buffer removed. Subsequently, 20 µl of 4% low-melting agarose was added, centrifuged at 3000 RPM for 10 min at 30 ˚C, and solidified by incubating for 15 min at 4 ˚C. The resulting pellet was transferred to a 27G needle and examined under a transmission electron microscope after washed 2-3 times with buffer.

Statistical analysis

Statistical significance between two different groups was calculated using Student's t-test. Results represent the mean±SD of three independent experiments. Experimental data $P<0.05$ ($^*P<0.05$, $^{**}P<0.01$, $^{***}P<0.001$, $^{****}P<0.0001$) were considered statistically significant.

Results

NE upregulates ROCK1 expression in rVSMCs

ROCK1 is typically expressed at low levels in rVSMCs under basal conditions. Our results demonstrated that both protein and mRNA expression of ROCK1 were significantly increased following NE treatment (Figure 1A-C). This

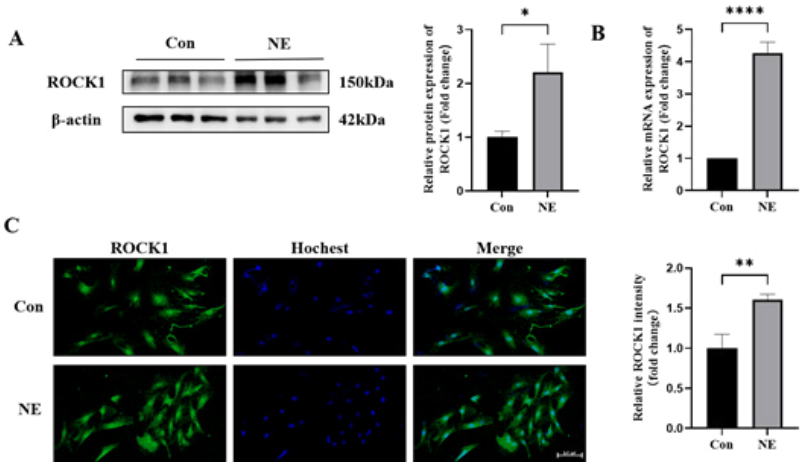

Figure 1. Expression of ROCK1 increases in rat vascular smooth muscle cells (rVSMCs) treated with Norepinephrine (NE)
A. Representative Western blot analysis of ROCK1 protein expression in rVSMCs after treatment with 30 µmol/L NE for 24 h. β-actin was used as a loading control. Quantification is shown on the right (n=3).* indicated $P<0.05$. (B) Relative mRNA expression of ROCK1 measured by quantitative real-time PCR (qRT-PCR) (n=3).**** indicated $P<0.0001$. (C) Immunofluorescence staining of ROCK1 (green) in rVSMCs. Nuclei were stained with Hoechst (blue). Quantification of fluorescence intensity is shown on the righ. Scale bar, 100 µm. ** indicated $P<0.01$. Con: Conrtrol; ROCK1: Rho-associated coiled-coil containing protein kinase 1

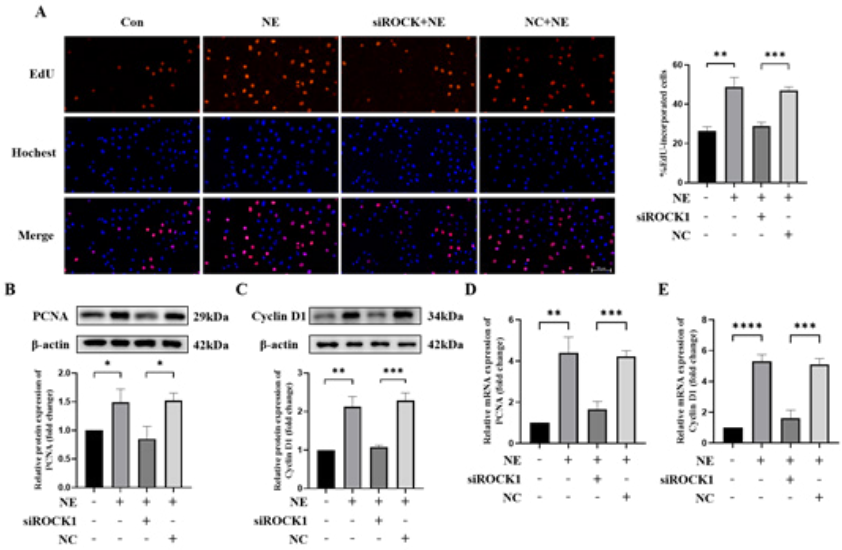

Figure 2. Down-regulation of ROCK1 inhibits rat vascular smooth muscle cells (rVSMCs) proliferation after induced by norepinephrine (NE)
A. Cell proliferation was evaluated by EdU staining assay (n=3). Scale bar, 50 μm. ** indicated P<0.01, *** indicated P<0.001. B-C. The protein levels of proliferation-related proteins, PCNA and Cyclin D1, were up-regulated in NE-treated rVSMCs and downregulated following ROCK1 knockdown (n=3). * indicated P<0.05, ** indicated P<0.01, *** indicated P<0.001. D-E. The mRNA levels of proliferation-related proteins PCNA and Cyclin D1 expression measured by quantitative real-time PCR up-regulated in NE-treated rVSMCs were downregulated following ROCK1 knockdown (n=3). *** indicated P<0.001, **** indicated P<0.0001
Con: Control; EdU: 5-Ethynyl-2'-deoxyuridine; ROCK: Rho-associated coiled-coil containing protein kinase1; PCNA: Proliferating Cell Nuclear Antigen; NC:Negative control

finding was further confirmed by immunofluorescence staining, which revealed enhanced ROCK1 expression in NE-treated cells (Figure 1D).

NE promotes rVSMCs proliferation via ROCK1

To investigate the role of ROCK1 in NE-induced cell proliferation, we first confirmed efficient ROCK1 knockdown by Western blotting (Figure S1A). EdU incorporation assays revealed that NE markedly enhanced rVSMCs proliferation, whereas this effect was significantly attenuated by ROCK1 knockdown (Figure 2A). Consistently, the expression of proliferative markers Proliferating Cell Nuclear Antigen (PCNA) and Cyclin D1 was up-regulated by NE but reduced after ROCK1 silencing, as shown by Western blot (Figure 2B, 2C) and real-time PCR analyses (Figure 2D, 2E). These results indicate that ROCK1 is essential for mediating NE-induced proliferation in rVSMCs.

NE enhances rVSMCs migration through ROCK1

Wound-healing assays showed that NE significantly promoted rVSMC migration at 24 hr compared with controls, whereas ROCK1 knockdown markedly suppressed this effect (Figure 3A). Mechanistically, NE treatment increased the expression of matrix metalloproteinases

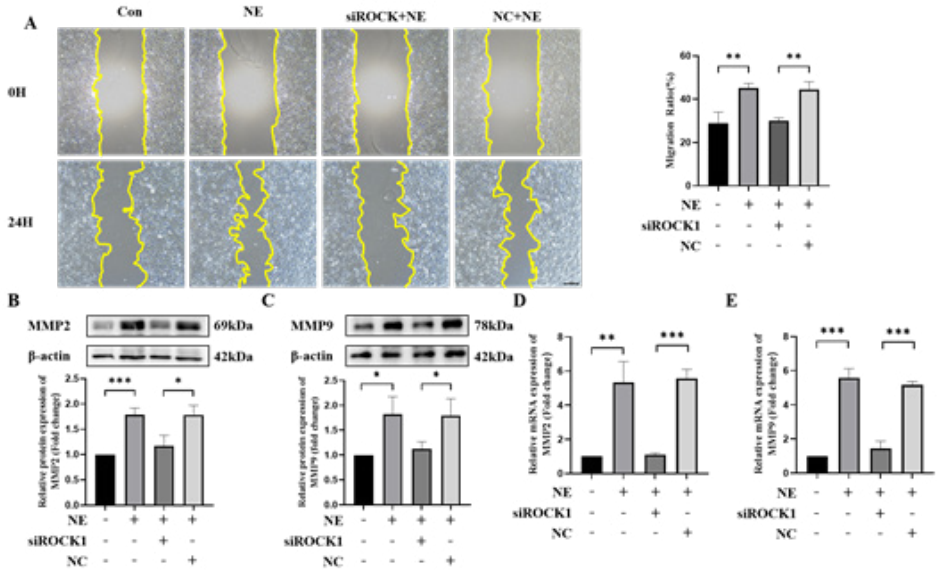

Figure 3. Down-regulation of ROCK1 inhibits rat vascular smooth muscle cells (rVSMCs) migration after induced by Norepinephrine (NE)
A. Cell migration was evaluated by wound healing assay (n=3). Scale bar, 200 μm. ** indicated P<0.01. B-C. The protein levels of migration-related proteins, MMP2 and MMP9, were up-regulated in NE-treated rVSMCs and downregulated following ROCK1 knockdown (n=3). * indicated P<0.05, *** indicated P<0.001. D-E. The mRNA levels of proliferation-related proteins, MMP2 and MMP9, were up-regulated in NE-treated rVSMCs and downregulated following ROCK1 knockdown (n=3). ** indicated P<0.01, *** indicated P<0.001
Con: Control; ROCK: Rho-associated coiled-coil containing protein kinase 1; MMP2: Matrix Metalloproteinase 2; MMP9: Matrix Metalloproteinase 9; NC: Negative control

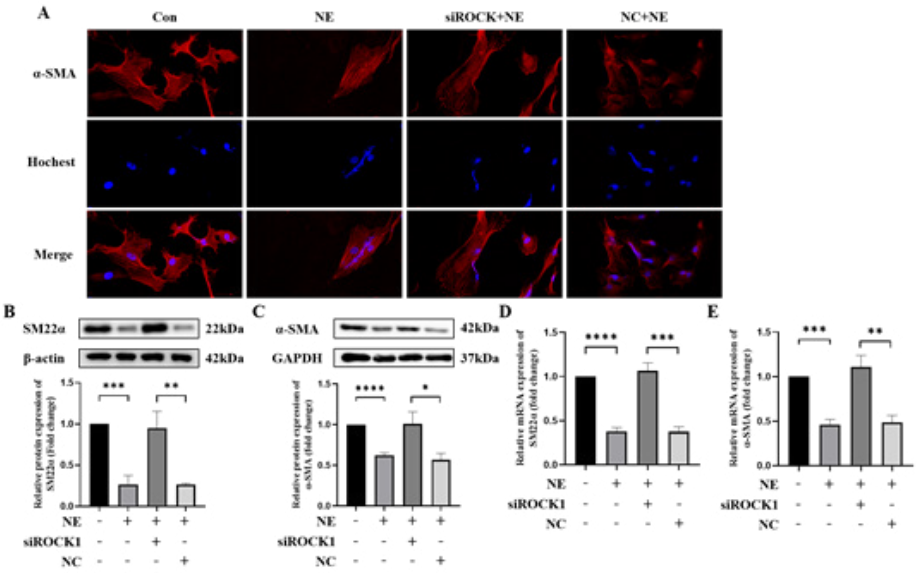

Figure 4. Down-regulation of ROCK1 inhibits rat vascular smooth muscle cells (rVSMCs) phenotype switch after induced by Norepinephrine (NE)
A. Phenotype switch was evaluated by Immunofluorescence staining. B-C. The protein levels of phenotype-related proteins SM22α and α-SMA, which were up-regulated in NE-treated rVSMCs, were downregulated following ROCK1 knockdown (n=3). * indicated $P<0.05$, ** indicated $P<0.01$, *** indicated $P<0.001$, **** indicated $P<0.0001$. D-E. The mRNA levels of proliferation-related proteins, MMP2 and MMP9, were up-regulated in NE-treated rVSMCs and downregulated following ROCK1 knockdown (n=3). ** indicated $P<0.01$, *** indicated $P<0.001$, **** indicated $P<0.0001$
Con: Control; ROCK: Rho-associated coiled-coil containing protein kinase 1; SM22α: Smooth Muscle Protein 22-α; α-SMA: α-smooth muscle actin; NC: Negative control

MMP-9 and MMP-2, key mediators of cellular migration (31, 32).ROCK1 knockdown effectively reversed this upregulation at both the protein (Figure 3B, 3C) and mRNA levels (Figure 3D, 3E). These findings demonstrate that ROCK1 contributes to NE-induced migration of rVSMCs, in part by regulating MMP-9 and MMP-2.

ROCK1 mediates NE-induced phenotypic switching of rVSMCs

SM22α and α-SMA are well-established markers of the contractile phenotype in VSMCs (33). Immunofluorescence staining showed that NE treatment significantly reduced α-SMA fluorescence intensity, whereas ROCK1 knockdown restored it (Figure 4A). Western blot analyses further revealed that NE decreased SM22α and α-SMA expression, which was partially rescued upon ROCK1 knockdown (Figure 4B, 4C). Real-time PCR confirmed consistent changes at the mRNA level (Figure 4D, 4E). These results indicate that ROCK1 plays a crucial role in mediating NE-induced phenotypic switching of rVSMCs from a contractile to a synthetic state.

NE regulates mitochondrial dynamics in rVSMCs

Mitochondria are highly dynamic organelles undergoing continuous fission and fusion, processes critical for VSMC phenotype regulation (34, 35). TEM analysis revealed increased mitochondrial division in NE-treated rVSMCs, accompanied by a dose-dependent reduction in mitochondrial area and circumference, and an elevated aspect ratio (Figure 5A). Despite these morphological changes, NE did not significantly alter the expression of the key fission mediator DRP1 (Figure 5B)(36, 37) or the fusion regulators MFN1 and OPA1 (Figure 5C, 5D)(38, 39). Interestingly, NE treatment induced a transient rise in cytoplasmic calcium levels (Figure 5E), suggesting a potential calcium-dependent mechanism underlying the observed mitochondrial fission.

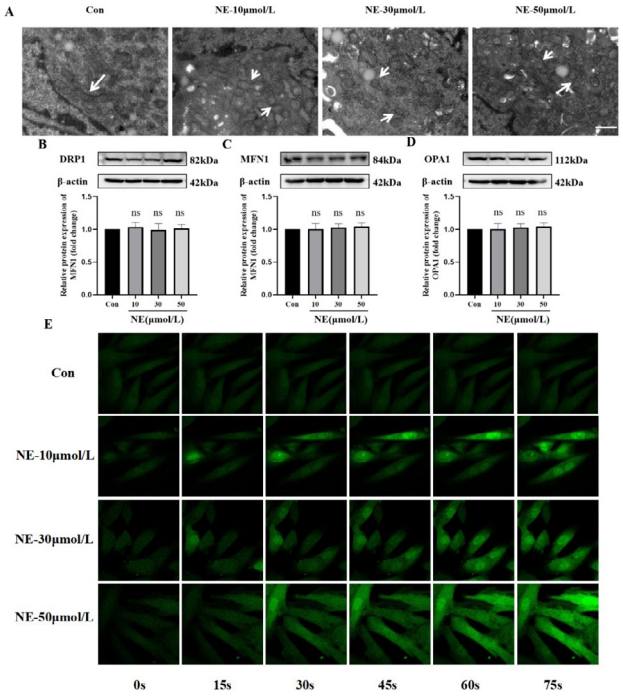

Figure 5. Norepinephrine (NE) promotes mitochondrial division and increases intracellular calcium ions
A. Following NE treatment, partial mitochondria were divided (indicated by white arrows). Scale bar=5 μm. B. DRP1 expression in cells treated with NE (24 h) for different durations(n=3). ns compared to the Control group C. MFN1 expression in cells treated with NE (24 h) for different durations (n=3). ns compared to the Control group D. OPA1 expression in cells treated with NE (24 h) for different durations (n=3). ns compared to the Control group E. NE induces an increase in mitochondrial cytoplasmic Ca^{2+} concentration
Con: Control; DRP1: Dynamin-related protein 1; MFN1: Mitofusin 1; OPA1: Optic Atrophy 1; ns: non-significant

Discussion

In this study, we identified a novel role for norepinephrine (NE) in promoting rVSMC proliferation, migration, and

phenotypic switching through activation of ROCK1. These findings extend previous evidence linking sympathetic overactivity with hypertensive nephropathy and vascular injury, and highlight ROCK1 as a critical mediator of renal vascular remodeling.

ROCK1 has long been implicated in cardiovascular and renal pathophysiology. Its activation increases vascular resistance, promotes extracellular matrix deposition, and contributes to glomerulosclerosis and tubulointerstitial fibrosis (20, 40, 41). Our results are consistent with these reports and further demonstrate that NE-induced ROCK1 activation drives the phenotypic transition of VSMCs from a contractile to a synthetic state. This switch was characterized by upregulation of proliferative and migratory markers, including PCNA, Cyclin D1, MMP-9, and MMP-2, underscoring ROCK1 signaling as a convergence point linking sympathetic hyperactivity to renal vascular remodeling in hypertensive nephropathy.

Beyond structural remodeling, our study provides the first evidence that NE influences mitochondrial dynamics in rVSMCs. NE treatment enhanced mitochondrial fission, in line with previous reports that excessive mitochondrial fragmentation contributes to vascular dysfunction and kidney injury (42, 43). Interestingly, the expression levels of canonical regulators of mitochondrial dynamics, such as DRP1, MFN1, and OPA1, were not significantly altered. This suggests that alternative pathways, possibly involving calcium signaling, may mediate NE-induced mitochondrial fission. Further investigation is needed to clarify this mechanism.

From a therapeutic standpoint, the NE–ROCK1 axis represents a promising target in hypertensive nephropathy. ROCK inhibitors such as fasudil and Y-27632 have demonstrated renoprotective effects in animal models by reducing fibrosis, improving renal hemodynamics, and attenuating proteinuria (44-46). Similarly, renal sympathetic denervation, which reduces circulating NE levels, has been shown to lower blood pressure and improve renal outcomes (47). Our findings provide a mechanistic rationale for these interventions and suggest that combining ROCK1 inhibition with approaches that modulate mitochondrial dynamics could provide synergistic benefits.

Nevertheless, several limitations must be acknowledged. First, the precise signaling mechanisms linking NE, calcium homeostasis, and mitochondrial fission remain unresolved. Second, our study was limited to in vitro cellular models; in vivo validation is necessary to confirm the physiological relevance of these findings. Finally, the potential crosstalk between ROCK1 signaling and other pathways, such as NF-κB or MAPK signaling, warrants further exploration.

In conclusion, we demonstrate that NE promotes rVSMCs proliferation, migration, phenotypic transformation, and mitochondrial dysfunction via ROCK1 activation, thereby contributing to the pathogenesis of hypertensive nephropathy. Targeting ROCK1 may represent a promising therapeutic strategy, and future studies should evaluate the efficacy of ROCK1 inhibitors and mitochondrial modulators in preclinical and clinical settings.

Conclusion

To our knowledge, this is the first study to demonstrate that norepinephrine (NE) regulates rVSMCs through ROCK1 signaling. We showed that NE upregulates ROCK1, thereby promoting rVSMCs proliferation, migration, and phenotypic switching, while simultaneously impairing mitochondrial homeostasis by reducing mitochondrial membrane potential and enhancing mitochondrial fission. Silencing ROCK1 effectively attenuated these pathological responses, underscoring its central role in NE-mediated vascular remodeling. These findings identify the NE–ROCK1 axis as a novel driver of hypertensive nephropathy and highlight ROCK1 inhibition as a potential therapeutic strategy. Future in vivo and clinical studies are needed to validate these mechanisms and explore the translational value of targeting ROCK1 in hypertensive vascular injury.

Acknowledgment

This work was supported by the National Natural Science Foundation of China (nos.82000397, 81900366), the First Affiliated Hospital of Harbin Medical University Funding program for training outstanding young medical talents (2021J03), and China Postdoctoral Science Foundation Project (2023MD744208).

Availability of Data and Material

Data utilized and analyzed in this study can be obtained from the corresponding author upon reasonable request.

Authors' Contributions

S C and L W designed the experiments; L W, H L, and J L performed experiments and collected data; S C and L W discussed the results and strategy; Y H and Y Z supervised, directed, and managed the study; M L and Y G approved the final version to be published.

Conflicts of Interest

The authors of this study declare that they have no competing financial interests or personal relationships that could have influenced the work presented.

Declaration

We acknowledge the use of ChatGPT 3.5 to enhance language quality and check for grammatical errors. After using this tool, we reviewed and edited the content as needed and take full responsibility for the content of the publication.

References

1. Leontsinis I, Mantzouranis M, Tsioufis P, Andrikou I, Tsioufis C. Recent advances in managing primary hypertension. Fac Rev 2020; 9: 4.
2. Burnier M, Damianaki A. Hypertension as cardiovascular risk factor in chronic kidney disease. Circ Res 2023; 132: 1050-1063.
3. Xie T, Bai Z, Chen Z, Liang H, Liu T, Lam LK, *et al.* Inhibition of ferroptosis ameliorates hypertensive nephropathy through p53/Nrf2/p21 pathway by Taohongsiwu decoction: Based on network pharmacology and experimental validation. J Ethnopharmacol 2023; 312: 116506.
4. Mancia G. Renal nerve ablation. Eur Heart J 2018; 39: 4060-4061.
5. Hoogerwaard AF, Elvan A. Is renal denervation still a treatment option in cardiovascular disease? Trends Cardiovasc Med 2020; 30: 189-195.
6. Isingrini E, Guinaudie C, Perret L, Guma E, Gorgievski V, Blum ID, *et al.* Behavioral and transcriptomic changes following brain-specific loss of noradrenergic transmission. Biomolecules 2023; 13: 511.
7. Slater C, Wang Q. Alzheimer's disease: An evolving

understanding of noradrenergic involvement and the promising future of electroceutical therapies. Clin Transl Med 2021; 11: e397.
8. Van Egroo M, Koshmanova E, Vandewalle G, Jacobs HIL. Importance of the locus coeruleus-norepinephrine system in sleep-wake regulation: Implications for aging and Alzheimer's disease. Sleep Med Rev 2022; 62: 101592.
9. Ma J, Li Y, Yang X, Liu K, Zhang X, Zuo X, *et al.* Signaling pathways in vascular function and hypertension: Molecular mechanisms and therapeutic interventions. Signal Transduct Target Ther 2023; 8: 168.
10. Brown IAM, Diederich L, Good ME, DeLalio LJ, Murphy SA, Cortese-Krott MM, *et al.* Vascular smooth muscle remodeling in conductive and resistance arteries in hypertension. Arterioscler Thromb Vasc Biol 2018; 38: 1969-1985.
11. Zhang J, Yin Z, Xu Y, Wei C, Peng S, Zhao M, *et al.* Resolvin E1/ChemR23 protects against hypertension and vascular remodeling in angiotensin II–induced hypertensive mice. Hypertension 2023; 80: 2650-2664.
12. Thompson JM, Landman J, Razorenova OV. Targeting the RhoGTPase/ROCK pathway for the treatment of VHL/HIF pathway-driven cancers. Small GTPases 2020; 11:32-38.
13. Barcelo J, Samain R, Sanz-Moreno V. Preclinical to clinical utility of ROCK inhibitors in cancer. Trends Cancer 2023; 9: 250-263.
14. King KE, Losier TT, Russell RC. Regulation of autophagy enzymes by nutrient signaling. Trends Biochem Sci 2021; 46: 687-700.
15. Li M, Lyu X, Liao J, Werth VP, Liu M-L. Rho Kinase regulates neutrophil NET formation that is involved in UVB-induced skin inflammation. Theranostics 2022; 12: 2133-2149.
16. Tang L, Dai F, Liu Y, Yu X, Huang C, Wang Y, *et al.* RhoA/ROCK signaling regulates smooth muscle phenotypic modulation and vascular remodeling via the JNK pathway and vimentin cytoskeleton. Pharmacol Res 2018; 133: 201-212.
17. Wang Y, Zheng XR, Riddick N, Bryden M, Baur W, Zhang X, *et al.* ROCK isoform regulation of myosin phosphatase and contractility in vascular smooth muscle cells. Circ Res 2009; 104: 531-540.
18. Fu P, Liu F, Su S, Wang W, Huang XR, Entman ML, *et al.* Signaling mechanism of renal fibrosis in unilateral ureteral obstructive kidney disease in ROCK1 knockout mice. J Am Soc Nephrol 2006; 17: 3105-3114.
19. Peng H, Li Y, Wang C, Zhang J, Chen Y, Chen W, *et al.* ROCK1 induces endothelial-to-mesenchymal transition in glomeruli to aggravate albuminuria in diabetic nephropathy. Sci Rep 2016; 6: 20304.
20. Zhang J, Chen S, Xiang H, Xiao J, Zhao S, Shu Z, *et al.* S1PR2/Wnt3a/RhoA/ROCK1/beta-catenin signaling pathway promotes diabetic nephropathy by inducting endothelial mesenchymal transition and impairing endothelial barrier function. Life Sci 2023; 328: 121853.
21. Huang C, Zhou Y, Huang H, Zheng Y, Kong L, Zhang H, *et al.* Islet transplantation reverses podocyte injury in diabetic nephropathy or induced by high glucose via inhibiting RhoA/ROCK/NF-kappaB signaling pathway. J Diabetes Res 2021; 2021: 9570405.
22. Liu S, Li X, Wen R, Chen L, Yang Q, Song S, *et al.* Increased thromboxane/prostaglandin receptors contribute to high glucose-induced podocyte injury and mitochondrial fission through ROCK1-Drp1 signaling. Int J Biochem Cell Biol 2022; 151: 106281.
23. Yuan N, Diao J, Dong J, Yan Y, Chen Y, Yan S, *et al.* Targeting ROCK1 in diabetic kidney disease: Unraveling mesangial fibrosis mechanisms and introducing myricetin as a novel antagonist. Biomed Pharmacother 2024; 171: 116208.
24. Liu X, Zhang W, Luo J, Shi W, Zhang X, Li Z, *et al.* TRIM21 deficiency protects against atrial inflammation and remodeling post myocardial infarction by attenuating oxidative stress. Redox Biol 2023; 62: 102679.
25. Keefe JA, Aguilar-Sanchez Y, Navarro-Garcia JA, Ong I, Li L, Paasche A, *et al.* Macrophage-mediated IL-6 signaling drives ryanodine receptor-2 calcium leak in postoperative atrial fibrillation. J Clin Invest 2025; 135: e187711.
26. Choi JH, Moon CM, Shin TS, Kim EK, McDowell A, Jo MK, *et al.* Lactobacillus paracasei-derived extracellular vesicles attenuate the intestinal inflammatory response by augmenting the endoplasmic reticulum stress pathway. Exp Mol Med 2020; 52: 423-437.
27. Fu J, Tang Y, Zhang Z, Tong L, Yue R, Cai L. Gastrin exerts a protective effect against myocardial infarction via promoting angiogenesis. Mol Med 2021; 27: 90.
28. Xiong G, Yun F, Jiang L, Yi Z, Yi X, Yang L, *et al.* NDUFS3 promotes proliferation via glucose metabolism reprogramming inducing AMPK phosphorylating PRPS1 to increase the purine nucleotide synthesis in melanoma. Cell Death Differ 2025; 32: 2193-2209.
29. Zhang L, Luo Y, Lv L, Chen S, Liu G, Zhao T. TRAP1 inhibits MARCH5-mediated MIC60 degradation to alleviate mitochondrial dysfunction and apoptosis of cardiomyocytes under diabetic conditions. Cell Death Differ 2023; 30: 2336-2350.
30. Ke M, Chong C-M, Zeng H, Huang M, Huang Z, Zhang K, *et al.* Azoramide protects iPSC-derived dopaminergic neurons with PLA2G6 D331Y mutation through restoring ER function and CREB signaling. Cell Death Dis 2020; 11: 130.
31. Chen X, Tian J, Zhao C, Wu Y, Li J, Ji Z, *et al.* Resveratrol, a novel inhibitor of fatty acid binding protein 5, inhibits cervical cancer metastasis by suppressing fatty acid transport into nucleus and downstream pathways. Br J Pharmacol 2024; 181: 1614-1634.
32. Xu W, Yao H, Wu Z, Yan X, Jiao Z, Liu Y, *et al.* Oncoprotein SET-associated transcription factor ZBTB11 triggers lung cancer metastasis. Nat Commun 2024; 15: 1362.
33. Furmanik M, Chatrou M, van Gorp R, Akbulut A, Willems B, Schmidt H, *et al.* Reactive oxygen-forming Nox5 links vascular smooth muscle cell phenotypic switching and extracellular vesicle-mediated vascular calcification. Circ Res 2020; 127: 911-927.
34. Li J, Li X, Song S, Sun Z, Li Y, Yang L, *et al.* Mitochondria spatially and temporally modulate VSMC phenotypes via interacting with cytoskeleton in cardiovascular diseases. Redox Biol 2023; 64: 102778.
35. Sun J, Shao Y, Pei L, Zhu Q, Yu X, Yao W. AKAP1 alleviates VSMC phenotypic modulation and neointima formation by inhibiting Drp1-dependent mitochondrial fission. Biomed Pharmacother 2024; 176: 116858.
36. Kraus F, Roy K, Pucadyil TJ, Ryan MT. Function and regulation of the divisome for mitochondrial fission. Nature 2021; 590: 57-66.
37. Quiles JM, Gustafsson ÅB. The role of mitochondrial fission in cardiovascular health and disease. Nat Rev Cardiol 2022; 19:723-736.
38. Gao S, Hu J. Mitochondrial fusion: The machineries in and out. Trends Cell Biol 2021; 31: 62-74.
39. Chandhok G, Lazarou M, Neumann B. Structure, function, and regulation of mitofusin-2 in health and disease. Biol Rev Camb Philos Soc 2017; 93: 933-949.
40. Siddiqui MR, Akhtar S, Shahid M, Tauseef M, McDonough K, Shanley TP. miR-144–mediated inhibition of ROCK1 protects against LPS-induced lung endothelial hyperpermeability. Am J Respir Cell Mol Biol 2019; 61: 257-265.
41. Lin D, Luo C, Wei P, Zhang A, Zhang M, Wu X, *et al.* YAP1 recognizes inflammatory and mechanical cues to exacerbate benign prostatic hyperplasia via promoting cell survival and fibrosis. Adv Sci (Weinh) 2024; 11: e2304274.
42. Mendez-Barbero N, Oller J, Sanz AB, Ramos AM, Ortiz A, Ruiz-Ortega M, *et al.* Mitochondrial dysfunction in the cardio-renal axis. Int J Mol Sci 2023; 24: 8209.
43. Li XL, Liu XW, Liu WL, Lin YQ, Liu J, Peng YS, *et al.* Inhibition of TMEM16A improves cisplatin-induced acute kidney injury via preventing DRP1-mediated mitochondrial fission. Acta Pharmacol Sin 2023; 44: 2230-2242.
44. Cavarape A, Endlich N, Assaloni R, Bartoli E, Steinhausen M, Parekh N, *et al.* Rho-kinase inhibition blunts renal vasoconstriction induced by distinct signaling pathways in vivo. J Am Soc Nephrol

2003; 14: 37-45.
45. Liu P, Huang W, Ding Y, Wu J, Liang Z, Huang Z, *et al.* Fasudil dichloroacetate alleviates SU5416/hypoxia-induced pulmonary arterial hypertension by ameliorating dysfunction of pulmonary arterial smooth muscle cells. Drug Des Devel Ther 2021; 15: 1653-1666.
46. Wang B, Wang Y, Tan Y, Guo J, Chen H, Wu PY, *et al.* Assessment of fasudil on contrast-associated acute kidney injury using multiparametric renal MRI. Front Pharmacol 2022; 13: 905547.
47. Vukadinovic D, Lauder L, Kandzari DE, Bhatt DL, Kirtane AJ, Edelman ER, *et al.* Effects of catheter-based renal denervation in hypertension: A systematic review and meta-analysis. Circulation 2024; 150: 1599-1611.